ACS Catalysis

Research Article

pubs.acs.org/acscatalysis

Preparation of Au/TiO_2 with Metal Cocatalysts Exhibiting Strong Surface Plasmon Resonance Effective for Photoinduced Hydrogen Formation under Irradiation of Visible Light

Atsuhiro Tanaka, Satoshi Sakaguchi, Keiji Hashimoto, and Hiroshi Kominami*

Department of Applied Chemistry, Faculty of Science and Engineering, Kinki University, Kowakae, Higashiosaka, Osaka 577-8502, Japan

Supporting Information

ABSTRACT: Titanium(IV) oxide (TiO_2) having both small platinum (Pt) nanoparticles and large gold (Au) particles without alloying and nanoparticle coagulation was successfully prepared by the combination of traditional photodeposition of Pt in the presence of a hole scavenger (PH) and subsequent Au colloid photodeposition in the presence of a hole scavenger (CPH) onto TiO_2−Pt. Au particles having an average diameter of 13 nm were fixed on both TiO_2 and TiO_2−Pt samples without change in the original size of Au particles, and the Au/TiO_2 and Au/TiO_2−Pt samples exhibited strong photoabsorption around 550 nm as a result of surface plasmon resonance (SPR) of Au to which the large size of Au particles was attributed. Bare TiO_2, TiO_2−Pt, Au/TiO_2, and Au/TiO_2−Pt samples were used for photoinduced hydrogen (H_2) formation from 2-propanol in aqueous solutions under irradiation of visible light. The first two samples yielded no H_2 because of no response to visible light, but the latter two formed H_2, indicating that SPR photoabsorption of supported Au particles contributed to the H_2 evolution under irradiation of visible light. The H_2 formation rate of the Au/TiO_2−Pt sample was ∼7-times larger than that of the Pt-free Au/TiO_2 sample, indicating that Pt nanoparticles loaded on TiO_2 acted effectively as a cocatalyst, that is, as reduction sites for H_2 evolution. The combination of the PH and CPH methods was effective for preparation of Au/TiO_2 having other metal cocatalysts (M) including Au, that is, Au/TiO_2−Au, and H_2 evolution rates decreased in the order of M; Pt > Pd > Ru > Rh > Au > Ag > Cu > Ir. An inverse correlation between the rate and the hydrogen overvoltage (HOV) of M, that is, it was observed that the higher the HOV, the more difficult it is to reduce protons by photogenerated electrons. Since the amounts of Au and M loaded on TiO_2 were changed independently, the effects on photoabsorption and the rate of H_2 evolution were examined. A linear correlation was observed between rate and light absorption due to SPR, suggesting that SPR photoabsorption by Au particles was one of the important factors determining the rate of the H_2 evolution.

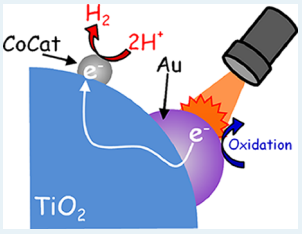

KEYWORDS: *photocatalyst, hydrogen formation, gold nanoparticles, surface plasmon resonance, visible light, cocatalyst*

1. INTRODUCTION

Hydrogen (H_2) production by semiconductor photocatalysts such as titanium(IV) oxide (TiO_2) has attracted much attention. It represents a promising technology to use renewable resources for clean and environmentally friendly energy production. TiO_2 is a wide band gap photocatalyst (band gap = 3.2 eV) that can induce evolution of H_2 from various compounds under ultraviolet (UV) light irradiation.[1−7] However, UV light accounts for only ∼5% of the total solar energy, whereas visible light accounts for ∼50% of total solar energy. Therefore, the development of photocatalysts using visible light is an important topic from a practical point of view. In recent years, results of extensive studies on H_2 formation over a visible light-responding photocatalyst have been reported.[8,9]

Recently, surface plasmon resonance (SPR) of gold (Au) nanoparticles has been applied to a visible light-responding photocatalyst;[10−27]however, there are limited reports on applications of SPR-induced photoabsorption to chemical reactions, that is, oxidation of organic substrates,[13,14,21−23,27] selective oxidation of aromatic alcohol to a carbonyl compound,[12,24,26] hydrogen formation from alcohols,[15,16,25] and selective reduction of organic compounds.[17] In our previous communication,[25] we reported the successful formation of H_2 from various compounds, including biomass-related compounds (2-propanol, methanol, ethanol, ammonia, and benzyl alcohol), in aqueous suspensions of Au/TiO_2 under visible light irradiation. By using a unique multistep photodeposition method,[23,25] Au/TiO_2 samples exhibiting stronger photoabsorption at around 550 nm due to SPR and higher levels of activity for H_2 production were successfully prepared. Two types of Au particles having different sizes were loaded onto TiO_2 in the samples, and it was concluded that the two types of Au nanoparticles had different functionalities; that is, the larger Au particles contributed to the strong light absorption, and the smaller Au particles acted as reduction sites for H_2 evolution. It is known that the rate of H_2 formation is greatly affected by the kind of cocatalyst loaded onto the

Received: October 1, 2012
Revised: November 23, 2012
Published: December 6, 2012

   dx.doi.org/10.1021/cs3006499 | ACS Catal. 2013, 3, 79−85

photocatalyst and that the effect of Au as a cocatalyst for H_2 formation is not so great.[5] Therefore, if efficient cocatalyst particles (optimally, nanoparticles) other than Au particles are loaded onto Au/TiO_2 exhibiting strong SPR, the Au/TiO_2 with the cocatalyst sample would show a large rate of H_2 formation under irradiation of visible light. However, loading both larger Au particles and smaller cocatalyst particles onto the TiO_2 surface without alloying or nanoparticle coagulation seems to be difficult.

Separately from the multistep photodeposition method, colloidal Au nanoparticles were successfully loaded onto TiO_2 without change in the original particle size using a method of colloid photodeposition operated in the presence of a hole scavenger (CPH).[27] The Au particles in the Au/TiO_2 samples prepared by the CPH method exhibited stronger SPR photoabsorption at around 550 nm due to the large particle size (13 nm). In this study, we examined preparation of TiO_2 samples on which large Au particles and small cocatalyst particles were loaded to satisfy both strong SPR absorption and efficient H_2 evolution under irradiation of visible light. Here, we report that Au/TiO_2 with cocatalyst samples were successfully prepared by a combination of the photodeposition method and CPH method and that the samples exhibited H_2 evolution rates larger than that of the cocatalyst-free Au/TiO_2 sample under irradiation of visible light.

2. EXPERIMENTAL SECTION

2.1. Synthesis of Nanocrystalline TiO_2. Nanocrystalline TiO_2 powder was prepared using the hydrothermal crystallization in organic media (HyCOM) method at 573 K.[28,29] Titanium(IV) butoxide and toluene were used as the starting material and solvent, respectively. The product was calcined at various temperatures for 1 h in a box furnace. The crystallinity of HyCOM-TiO_2 samples was improved by calcination, and the samples still possessed a large specific surface area of 97 $m^2\ g^{-1}$, even after calcination at 723 K. The TiO_2 sample calcined at 723 K was used in most of the experiments as a supporting material for Au particles and is shown hereafter simply as TiO_2. When the HyCOM-TiO_2 samples obtained by calcination at various temperatures were used, the temperature is shown in parentheses after TiO_2; for example, TiO_2 calcined at 973 K is designated as TiO_2(973).

2.2. Loading of Cocatalysts on TiO_2. Loading of cocatalysts (M) on TiO_2 (preparation of TiO_2−M) was performed by the photodeposition with hole scavenger (PH) method. TiO_2 powder was suspended in 10 cm^3 of an aqueous solution of methanol (50 vol %) in a test tube, and the test tube was sealed with a rubber septum under argon (Ar). An aqueous solution of the cocatalyst source was injected into the sealed test tube and then photoirradiated for 2 h at $\lambda > 300$ nm by a 400 W high-pressure mercury arc (Eiko-sha, Osaka) with magnetic stirring in a water bath continuously kept at 298 K. The cocatalyst source was reduced by photogenerated electrons, and metal was deposited on the surface of the TiO_2 particles. Analysis of the liquid phase after photodeposition revealed that the cocatalyst source had been almost completely (>99.9%) deposited on the TiO_2 particles. The resultant powder was washed repeatedly with distilled water and then dried at 310 K overnight under air.

2.3. Preparation of Au Particles and Loading of Au Particles on TiO_2−M. Colloidal Au nanoparticles were prepared using the method reported by Frens.[30] To 750 cm^3 of an aqueous tetrachloroauric acid ($HAuCl_4$) solution (0.49 mmol dm^{-3}), 100 cm^3 of an aqueous solution containing sodium citrate (39 mmol dm^{-3}) was added. The solution was heated and boiled for 1 h. After the color of the solution had changed from deep blue to deep red, the solution was boiled for an additional 30 min. After the solution was cooled to room temperature, Amberlite MB-1 (ORGANO, 60 cm^3) was added to remove excess sodium citrate. After 1 h of treatment, MB-1 was removed from the solution using a glass filter. Loading of Au particles on the TiO_2−M samples was performed by the CPH method.[27] Preparation of TiO_2−M having 1.0 wt % Au as a typical sample is described. A TiO_2−M sample (168 mg) was suspended in 20 cm^3 of an aqueous solution of colloidal Au nanoparticles (0.085 mg cm^{-3}) in a test tube, and the test tube was sealed with a rubber septum under Ar. An aqueous solution of oxalic acid (50 μmol) was injected into the sealed test tube. The mixture was photoirradiated at $\lambda > 300$ nm by a 400 W high-pressure mercury arc under Ar with magnetic stirring in a water bath continuously kept at 298 K. The resultant powder was washed repeatedly with distilled water and then dried at 310 K overnight under air. Co-catalyst-free samples (Au/TiO_2) were also prepared by the same method using bare TiO_2 samples. When samples with different Au contents were prepared, the amount of TiO_2−M (or TiO_2) was changed (volume and concentration of the Au colloidal solution being fixed). Hereafter, a Au-loaded TiO_2−M sample having X wt % of M and Y wt % of Au is designated as Au(Y)/TiO_2−M(X); for example, a sample having 0.5 wt % platinum (Pt) and 1.0 wt % Au is shown as Au(1.0)/TiO_2−Pt(0.5).

2.4. CHARACTERIZATION

Diffuse reflectance spectra of the samples were obtained with a UV−visible spectrometer (UV-2400, Shimadzu, Kyoto) equipped with a diffuse reflectance measurement unit (ISR-2000, Shimadzu). X-ray diffraction (XRD) patterns of the samples were recorded using a Rigaku Multi Flex (Cu Kα, 40 V, 30 mA) with a carbon monochromator. Diffraction patterns were obtained in the angle range from 20° to 70°. Morphology of the samples was observed under a JEOL JEM-3010 transmission electron microscope (TEM) operated at 300 kV in the Joint Research Center of Kinki University. Specific surface areas of the TiO_2 samples were determined using the BET single-point method on the basis of nitrogen uptake measured at 77 K.

2.5. PHOTOCATALYTIC ACTIVITY TEST

In this study, the formation of H_2 and acetone from 2-propanol over photocatalyst under irradiation of visible light was chosen as the test reaction, as expressed in eq 1.

$$(CH_3)_2CHOH \rightarrow (CH_3)_2CO + H_2 \quad (1)$$

The dried photocatalyst powder (50 mg) was suspended in 50 vol % 2-propanol/water solution (5 cm^3), bubbled with Ar, and sealed with a rubber septum. The suspension was irradiated with visible light of a 500 W xenon (Xe) lamp (Ushio, Tokyo) filtered with a Y-48 filter (AGC Techno Glass) (450−600 nm: 83 mW cm^{-2}) with magnetic stirring in a water bath continuously kept at 298 K. The amount of H_2 in the gas phase was measured using a Shimadzu GC-8A gas chromatograph equipped with an MS-5A column. The amount of acetone in the liquid phase was determined with a Shimadzu GC-14A gas chromatograph equipped with a fused-silica capillary column (HiCap-CBP20, 25 m, 0.22 mm). Toluene

dx.doi.org/10.1021/cs3006499 | ACS Catal. 2013, 3, 79−85

was used as an internal standard sample. The reaction solution (1 cm^3) was added to a diethyl ether/water mixture (2:1 v/v, 3 cm^3). After the mixture had been stirred for 10 min, acetone in the ether phase was analyzed. The amount of acetone was determined from the ratio of the peak area of acetone to the peak area of toluene.

3. RESULTS AND DISCUSSION

3.1. TEM Observation. Figure 1a shows a TEM photograph of the TiO_2−Pt(0.5) sample simply prepared by the traditional PH method. Small Pt particles were observed, and the average diameter was determined to be 3.2 nm, indicating that the Pt nanoparticles were successfully deposited on the surface of TiO_2 by using the PH method. Figure 1b shows a TEM photograph and distribution of colloidal Au nanoparticles, revealing that Au nanoparticles have an average particle size of 13 nm within a relatively sharp distribution with a standard deviation of 1.4 nm. Figure 1c shows a TEM image of Au(1.0)/TiO_2 prepared by the CPH method using the Au colloidal solution. Gold particles were observed in the image, indicating that Au nanoparticles were deposited on the TiO_2 surface by the CPH method.

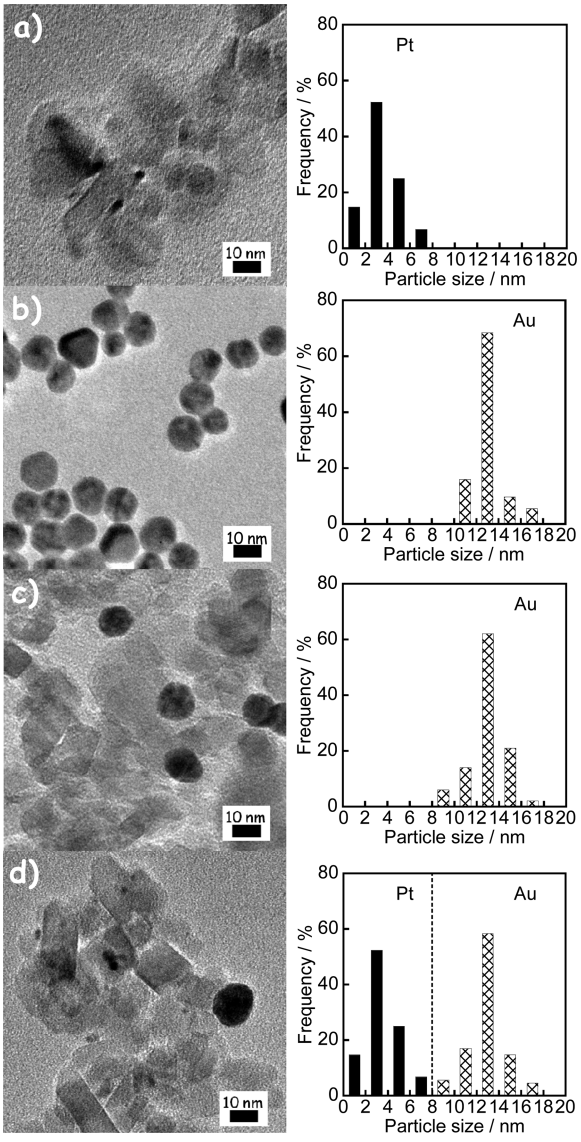

Figure 1. TEM photographs (left) and size distributions (right) of (a) TiO_2−Pt(0.5), (b) colloidal Au nanoparticles, (c) Au(1.0)/TiO_2, and (d) Au(1.0)/TiO_2−Pt(0.5).

The average diameter of Au particles of the sample was determined to be 13 nm, which was in good agreement with the average diameter of original colloidal Au nanoparticles before Au loading (Figure 1b). In the TEM photograph of the Au(1.0)/TiO_2−Pt(0.5) sample (Figure 1d), both smaller and larger particles were observed, and the average diameters were determined to be 3.8 and 13 nm, respectively. From the TEM photographs of TiO_2−Pt(0.5) and Au(1.0)/TiO_2 samples, the smaller and larger particles of the Au(1.0)/TiO_2−Pt(0.5) sample were assigned to Pt and Au, respectively. These results indicate that the CPH method induced no change in Pt nanoparticles during loading of Au particles and that Au nanoparticles were successfully loaded onto TiO_2−Pt without a change in the original particle size, as in the case of the loading of Au onto bare TiO_2.

In our previous study using the CPH method, we found that the presence of a hole scavenger was indispensable for quantitative loading of Au particles; that is, a reductive condition should be created on the TiO_2 surface.[27] Therefore, in the case of loading of Au particles on TiO_2−Pt by the CPH method, Au particles would be deposited in contact with Pt nanoparticleas because Pt particles loaded onto TiO_2 often act as reduction sites in various reaction systems. The numbers of Pt and Au particles in TiO_2−Pt(0.5) and Au(1.0)/TiO_2 samples were calculated to be 1.4×10^{16} and 5.6×10^{13} per g of TiO_2, respectively, from the average sizes, contents, and densities of Pt and Au, assuming that both Pt and Au particles were spherical. Since the number of Pt particles was much larger than that of Au particles, the decrease in the number of exposed Pt particles due to contact with Au particles by the CPH method is negligible in the Au(1.0)/TiO_2−Pt(0.5) sample.

3.2. Photoabsorption Properties. Figure 2 shows absorption spectra of the TiO_2, TiO_2−Pt(0.5), Au(1.0)/TiO_2, and Au(1.0)/TiO_2−Pt(0.5) samples for which TEM photographs are shown in Figure 1. The bare TiO_2 sample exhibited an absorption only at $\lambda < 400$ nm because of the band gap excitation. Loading Pt nanoparticles onto TiO_2 resulted in an increase in the baseline of photoabsorption that has generally been observed as a change in color from white to gray. In the spectra of Au(1.0)/TiO_2 and Au(1.0)/TiO_2−Pt(0.5) samples, strong photoabsorption was observed at around 550 nm, which was attributed to SPR of the supported Au nanoparticles.[10−27] Since photoabsorption due to Pt particles was also included, the

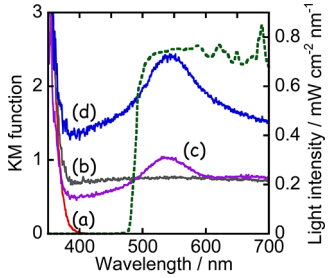

Figure 2. Absorption spectra of (a) TiO_2, (b) TiO_2−Pt(0.5), (c) Au(1.0)/TiO_2, and (d) Au(1.0)/TiO_2−Pt(0.5) and visible light irradiated to reaction systems (2-propanol in aqueous suspensions of photocatalysts) from a Xe lamp with a Y-48 filter.

dx.doi.org/10.1021/cs3006499 | ACS Catal. 2013, 3, 79−85

Au(1.0)/TiO_2–Pt(0.5) sample exhibited stronger photoabsorption.

3.3. Photocatalytic Activity Test. TiO_2, TiO_2–Pt(0.5), Au(1.0)/TiO_2, and Au(1.0)/TiO_2–Pt(0.5) samples were used for formation of H_2 from 2-propanol in their aqueous suspensions under visible light irradiation from a Xe lamp with a Y-48 filter at 298 K. Visible light irradiated to the reaction system is shown in Figure 2. Rates of H_2 evolution are shown in Figure 3. No H_2 was evolved in the case of either

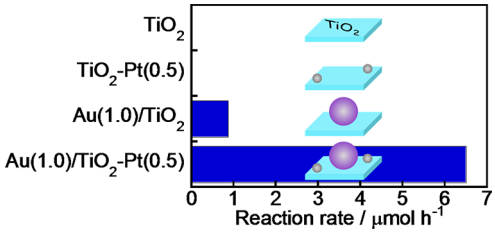

Figure 3. Rates of formation of H_2 from 2-propanol in aqueous suspensions of various photocatalysts under irradiation of visible light from a Xe lamp with a Y-48 cut-filter.

TiO_2 or TiO_2–Pt(0.5). These results indicate that visible light coming from a filtered Xe lamp did not cause band gap excitation of TiO_2 and that photocatalysis and/or thermocatalysis of TiO_2–Pt(0.5) were negligible under the present conditions. On the other hand, the Au(1.0)/TiO_2 sample was active in H_2 formation and showed an H_2 evolution rate of 0.87 μmol h^{-1}. However, the rate was much smaller than that of the Au/TiO_2 sample (2.7 μmol h^{-1}) prepared by the multistep (MS) photodeposition method on which two types of Au particles having different sizes were loaded.[25] The main difference in the MS- and CPH-Au/TiO_2 samples was whether small Au particles existed. In our previous paper on photocatalytic activity of MS-Au/TiO_2 samples,[25] we concluded that the two types of Au nanoparticles had different functionalities; that is, the larger Au particles contributed to the strong light absorption, and the smaller Au particles acted as reduction sites for H_2 evolution. Therefore, lack of small Au particles, that is, insufficient functionality in the reduction sites, would be attributed to the smaller rate of H_2 formation of the CPH-Au/TiO_2 sample, and the sample would show a large rate of H_2 formation if efficient cocatalyst particles (optimally nanoparticles) are loaded. As expected, the Au(1.0)/TiO_2–Pt(0.5) sample exhibited a much larger H_2 formation rate of 6.5 μmol h^{-1}, indicating that Pt particles loaded onto TiO_2 effectively acted as reduction sites for H_2 evolution. Loading both larger Au particles and smaller cocatalyst particles on the TiO_2 surface without alloying or nanoparticle coagulation has been difficult, as stated above. This requisite was successfully achieved, and a large reaction rate was obtained, as predicted, by the Au(1.0)/TiO_2–Pt(0.5) sample prepared by combination of the traditional PH method for small Pt cocatalyst particles and the CPH method for large Au particles.

3.4. Effects of Cocatalysts. Various cocatalysts were loaded onto TiO_2 by using the PH method, and then Au particles were fixed on TiO_2–M by using the CPH method. The Au(1.0)/TiO_2–M(0.5) samples were used for evolution of H_2 from 2-propanol in aqueous suspensions of various photocatalysts under visible light irradiation, and the effects of M on reaction rates were compared. In this study, iridium (Ir, chloride), copper (Cu, chloride), silver (Ag, sulfate), gold (Au, tetrachloroauric acid), rhodium (Rh, chloride), ruthenium (Ru, chloride), and palladium (Pd, chloride) as well as Pt were used as the cocatalysts and sources. TEM observation revealed that the average particle sizes of the cocatalysts were almost the same (Figure S1, Supporting Information), suggesting that surface areas of the cocatalysts in the Au(1.0)/TiO_2–M(0.5) samples were similar.

The rates of H_2 formation are shown in Figure 4. The H_2 formation rates of all samples with cocatalysts prepared in this

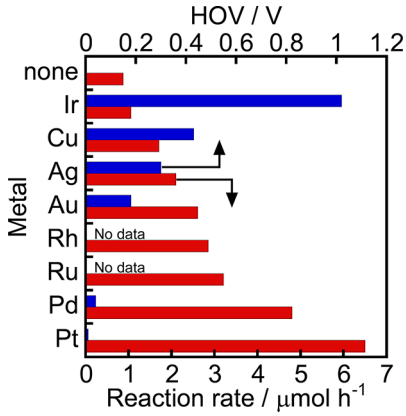

Figure 4. Effect of metal cocatalysts (M) on the rate of production of H_2 from 2-propanol in aqueous suspensions of Au(1.0)/TiO_2–M(0.5) samples (bottom) and hydrogen overvoltage (HOV) of electrodes composed of M (top).

study were larger than that of the M-free Au(1.0)/TiO_2 sample. Among the cocatalysts used in this study, Pt exhibited the greatest effect on H_2 evolution, and the rates of the Au(1.0)/TiO_2–M(0.5) samples decreased in the order, M = Pt > Pd > Ru > Rh > Au > Ag > Cu > Ir. This order reminded us of hydrogen overvoltage (HOV) of electrodes composed of each metal, and HOV data were inserted in Figure 4, although some HOV data were not found.[5,31] An inverse correlation between the rates and HOV values was observed: that is, the higher the HOV is, the more difficult it is to reduce protons (H^+) by electrons. These results indicate that each cocatalyst in the Au(1.0)/TiO_2–M(0.5) sample actually acted as a site for H^+ reduction (H_2 formation). It should be noted that the Au(1.0)/TiO_2–Au(0.5) sample in which two types of Au particles were loaded onto TiO_2 exhibited a larger rate than that of the Au(1.0)/TiO_2 sample, indicating that smaller Au nanoparticles loaded by the PH method worked efficiently as a cocatalyst.

In our previous study, a TiO_2–Au(0.5) sample free from colloidal Au particles was prepared by using the PH method and the sample exhibited a very low H_2 formation rate (0.44 μmol h^{-1}) under the same conditions.[25] Therefore, the results obtained for Au(1.0)/TiO_2–Au(0.5), Au(1.0)/TiO_2, and TiO_2–Au(0.5) support our conclusion in the previous paper[25] that the two types of Au nanoparticles had different functionalities; that is, the larger Au particles contributed to the strong light absorption, and the smaller Au particles acted as reduction sites for H_2 evolution.

3.5. Effect of Amount of Pt Cocatalyst. To examine the effect of the amount of Pt cocatalyst on the rate of H_2 formation, TiO_2–Pt(X) samples having various Pt loadings (X) were prepared, and then Au particles (1.0 wt %) were introduced to the samples by using the CPH method. The Au(1.0)/TiO_2–Pt(X) samples were used for H_2 formation

dx.doi.org/10.1021/cs3006499 | ACS Catal. 2013, 3, 79–85

from aqueous solutions of 2-propanol under irradiation of visible light; the rates of H_2 formation are shown in Figure 5a.

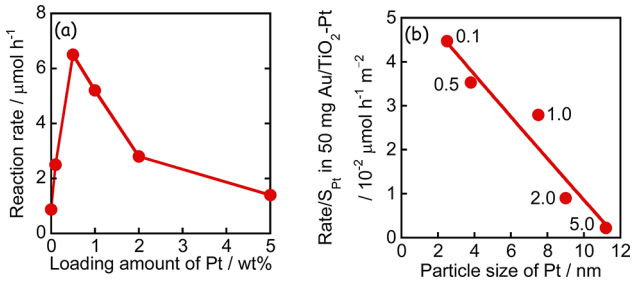

Figure 5. (a) Effect of Pt loading amounts (X) on the rate of evolution of H_2 from 2-propanol in aqueous suspensions of Au(1.0)/TiO_2–Pt(X) samples under irradiation of visible light and (b) effect of size of Pt particles on rate per surface area of Pt particles in 50 mg Au(1.0)/TiO_2–Pt(X) samples (rate/S_{Pt}). Values are Pt loading amounts (X).

The Pt-free sample (Au(1.0)/TiO_2) exhibited a small rate of H_2 formation (0.87 μmol h^{-1}), as shown earlier. Only a small amount of Pt loading (X = 0.1 wt %) increased the rate, indicating that Pt nanoparticles effectively acted as the reduction center in the sample. The reaction rate increased until X = 0.5 wt %, and further increase in X decreased the rate. Totally, the maximum rate of H_2 formation (6.5 μmol h^{-1}) was obtained at X = 0.5 wt %. The average size of Pt nanoparticles (D_{Pt}) in Au(1.0)/TiO_2–Pt(X) was determined by TEM. Fine Pt particles of less than 4 nm in diameter were loaded onto TiO_2 when the amount of Pt was small (X = 0.1 and 0.5 wt %); however, the value of D_{Pt} drastically increased to 7.8 nm at X = 1.0 wt %, indicating that the PH method was suitable for loading a small amount of fine particles on TiO_2. The external surface area of Pt particles in 50 mg of Au(1.0)/TiO_2–Pt(X) (S_{Pt}) was calculated from D_{Pt}, and then the reaction rate per S_{Pt} (rate/S_{Pt}) was plotted against D_{Pt} (Figure 5b). The value of rate/S_{Pt} monotonically decreased with the increase in D_{Pt}. These results support the idea that the Pt particles acted as reduction sites in the Au(0.5)/TiO_2–Pt(X) samples and suggest that the reaction is structure sensitive on Pt particles.

3.6. Effect of Amount of Au Particles. To examine the effect of the amount of Au on the rate of H_2 formation, various amounts of Au (Y) were loaded onto the TiO_2–Pt(0.5) sample by using the CPH method. The Au(Y)/TiO_2–Pt(0.5) samples were used for H_2 formation from aqueous solutions of 2-propanol under irradiation of visible light, and the rates of H_2 formation are shown in Figure 6a. The amount of H_2 increased linearly with photoirradiation time in all Au(Y)/TiO_2–Pt(0.5) samples, and the reaction rates were determined from the slopes of time–H_2 evolution plots. The rate of H_2 formation increased almost linearly with increase in Y until Y = 1.0 wt % and gradually increased after Y = 1.0 wt %. Figure 6a also shows the effect of the amount of Au loading (Y) on light absorption due to SPR at 550 nm. Since TiO_2–Pt(0.5) exhibited broad photoabsorption (Figure 2), light absorption at 550 nm was obtained by subtracting [1-reflection] of TiO_2–Pt(0.5) at 550 nm from that of Au(1.0)/TiO_2–Pt(0.5) at 550 nm. The light absorption due to SPR at 550 nm increased with increase in Y until Y = 1.0 wt % and gradually increased after Y = 1.0 wt %. The Y dependency of light absorption due to SPR was similar to that of the reaction rate, and a linear correlation was observed between the reaction rate and the light absorption due to SPR (Figure 6b), suggesting that SPR photoabsorption by

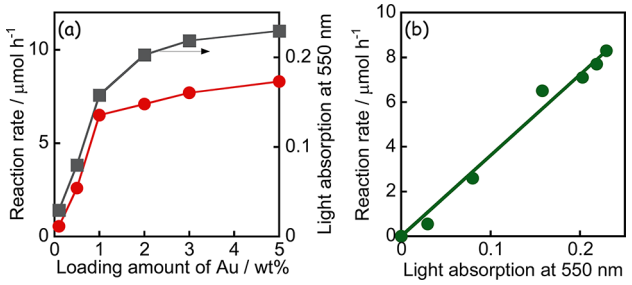

Figure 6. (a) Effects of Au loading amounts (Y) on the rate of evolution of H_2 from 2-propanol in aqueous suspensions of Au(Y)/TiO_2–Pt(0.5) samples under irradiation of visible light (left axis) and on light absorption at 550 nm (right axis) and (b) correlation between light absorption at 550 nm and rate of evolution of H_2.

Au particles was one of the important factors determining the rate of H_2 evolution. A similar result has been obtained in Ag/TiO_2 photocatalyst under irradiation of UV light.[32]

3.7. Action Spectrum. An action spectrum is a strong tool for determining whether an observed reaction occurs via a photoinduced process or a thermocatalytic process. To obtain an action spectrum in this reaction system, H_2 formation from 2-propanol in an aqueous suspension of Au(1.0)/TiO_2–Pt(0.5) was carried out at 298 K under irradiation of monochromated visible light from a Xe lamp with light width of ±5 nm. Apparent quantum efficiency (AQE) at each centered wavelength of light was calculated from the ratio of the double amount of H_2 and the amount of photons irradiated using the following equation:

$$\mathrm{AQE} = \frac{2 \times \text{the amount of hydrogen}}{\text{the amount of incident photons}} \times 100$$

As shown in Figure 7, AQE was in agreement with the subtraction spectrum obtained from the spectra of Au(1.0)/

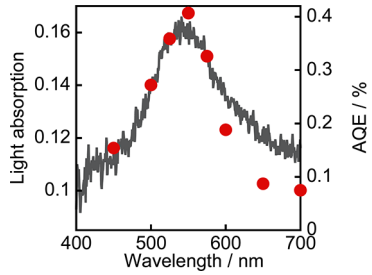

Figure 7. Subtraction spectrum obtained from spectra of Au(1.0)/TiO_2–Pt(0.5) and TiO_2–Pt(0.5) measured with barium sulfate as a reference (left axis) and action spectrum of Au(1.0)/TiO_2–Pt(0.5) (circles) in formation of H_2 from 2-propanol (right axis).

TiO_2–Pt(0.5) and TiO_2–Pt(0.5). Therefore, it can be concluded that H_2 formation from 2-propanol in an aqueous suspension of Au(1.0)/TiO_2–Pt(0.5) was induced by photoabsorption due to SPR of Au supported on TiO_2. We noted that AQE reached 0.41% at 550 nm and 0.075% even at 700 nm under the above conditions in the case of Au(1.0)/TiO_2–Pt(0.5).

3.8. Effect of Type of TiO_2. To examine the effect(s) of physical properties and crystal structure, HyCOM-TiO_2 samples calcined at various temperatures and representative commercial TiO_2 samples were used as supports for Au particles in the absence and presence of Pt particles. Pt and Au

dx.doi.org/10.1021/cs3006499 | ACS Catal. 2013, 3, 79–85

Table 1. Specific Surface Areas and Crystal Structures of Various TiO_2 Samples and H_2 Evolution from 2-Propanol in Aqueous Suspensions of Au/TiO_2 and Au/TiO_2−Pt under Irradiation of Visible Light

			Au(1.0)/TiO_2			Au(1.0)/TiO_2−Pt(0.5)			
TiO_2 and SnO_2[a]	S_{BET} /m^2g^{-1}[b]	crystal structure[c]	$Y(H_2)$[d]/μmol	$Y(Ac)$[e]/μmol	$Y(H_2)/Y(Ac)$	$Y(H_2)$[d]/μmol	$Y(Ac)$[e]/μmol	$Y(H_2)/Y(Ac)$	AQE[f]/%
TiO_2(723)	97	A	8.9	8.6	1.0	64	66	0.97	0.41
TiO_2(823)	91	A	7.1	7.6	0.93	56	54	1.0	0.34
TiO_2(973)	54	A	4.8	4.7	1.0	29	28	1.0	0.17
TiO_2(1073)	31	A	3.3	3.5	0.94	24	26	0.92	0.16
TiO_2(1173)	13	A, R	0.71	0.88	0.88	6.0	4.8	1.3	0.040
TiO_2(1273)	2.3	R	trace	trace		trace	trace		
P25	50	A, R	6.4	6.8	0.94	35	36	0.97	0.20
ST-01	338	A	5.1	4.8	1.1	27	24	1.1	0.17
MT-150A	93	R	trace	trace		trace	trace		
SnO_2	45		trace	trace		trace	trace		

[a]TiO_2 was synthesized by the HyCOM method and calcined at the temperature (K) shown in parentheses. P25, ST-01, and MT-150A were supplied by Degussa, Ishihara, and Tayca, respectively. SnO_2 was supplied by Nanotek. [b]BET surface area. [c]A, anatase; R, rutile. [d]H_2 yield for 10 h. [e]Acetone yield for 10 h. For both footnotes d and e, 50 mg of photocatalyst and visible light in the range of 450−600 nm (83 mW cm^{-2})was used. [f]Apparent quantum efficiency; 50 mg of photocatalyst and monochromated visible light from a Xe lamp with light width of ±5 nm (0.4 mW cm^{-2} at 550 nm).

particles were loaded by the PH and CPH methods, respectively. The amounts of Pt and Au were fixed at 0.5 wt % and 1.0 wt %, respectively, and various Au/TiO_2 and Au/TiO_2−Pt samples were used for H_2 evolution from 2-propanol under irradiation of visible light. Table 1 summarizes yields of H_2 in the gas phase and acetone in the liquid phase after 10 h of irradiation as well as specific surface area and the crystalline phase of TiO_2. In all anatase-type TiO_2 and anatase-rutile-mixed TiO_2 samples, H_2 and acetone were formed and the activities of the Au/TiO_2 and Au/TiO_2−Pt samples roughly depended on the specific surface area. The yields of H_2 reached 8.9 μmol in the case of Au(1.0)/TiO_2(723) and 64 μmol in the case of Au(1.0)/TiO_2(723)−Pt(0.5), whereas the yields of acetone in the liquid phase were 8.6 and 66 μmol, respectively. The ratios of the amount of H_2 formation to the amount of acetone over various Au(1.0)/TiO_2 and Au(1.0)/TiO_2−Pt(0.5) samples are also shown in Table 1. Values around unity were obtained in all of the anatase-type TiO_2 and anatase−rutile-mixed TiO_2 samples. Therefore, good agreement with yields of H_2 and acetone in these samples shows that stoichiometric dehydrogenation of 2-propanol occurred as expressed in eq 1.

The activities of Au(1.0)/TiO_2−Pt(0.5) samples were 5−9 times higher than those of Pt-free Au(1.0)/TiO_2 samples, indicating that Pt particles worked effectively as reduction sites for H_2 evolution, regardless of the physical properties. In contrast with these TiO_2 samples, H_2 evolution was negligible from 2-propanol in aqueous suspensions of rutile-type TiO_2 and SnO_2 samples. Since the conduction band of rutile-type TiO_2 and SnO_2 is lower than that of anatase-type TiO_2, the position of the conduction band of the TiO_2 support seems to be important for Au/TiO_2 and Au/TiO_2−Pt in H_2 evolution under the present reaction conditions. Table 1 also shows AQE values over various Au(1.0)/TiO_2−Pt(0.5) samples (AQE) under irradiation of monochromated visible light from a Xe lamp with light width of ±5 at 550 nm. Among these samples, the TiO_2(723) sample showed the highest AQE value (0.41%). This value was larger than the reported value for Au/TiO_2 (0.26%) at λ = 510−740 nm in H_2 formation from an ethanol solution.[27]

3.9. Expected Working Mechanism. The expected working mechanism for H_2 formation from aqueous solutions of 2-propanol over Au/TiO_2−M under irradiation of visible light is shown in Figure 8. Rapid electron transfer from Au to the TiO_2 film under visible light irradiation was observed using femtosecond transient absorption spectroscopy.[11] Four processes occur: (1) the incident photons are absorbed by Au particles through their SPR excitation, (2) electrons are injected from the Au particles into the conduction band of TiO_2, (3) the resultant electron-deficient Au particles oxidize 2-propanol to acetone and return to their original metallic state, and (4) electrons in the conduction band of TiO_2 transfer to the metal cocatalyst at which reduction of H^+ to H_2 occurs. The linear correlation between light absorption and the rate of H_2 formation (Figure 6b) and dependency of the rate of H_2 formation on the metal cocatalyst (Figure 4) support the working mechanism and indicate the importance of processes 1, 2, and 4. Electron transfer from Au particles to cocatalyst via TiO_2 suggests that the conduction band of TiO_2 bends at the TiO_2−Au interface and electrons transfer to cocatalyst particles as a result of the electric field gradient.

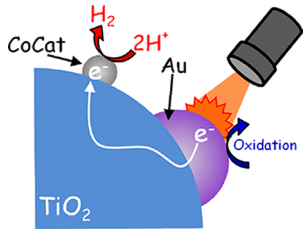

Figure 8. Expected reaction mechanism for production of H_2 from 2-propanol in aqueous suspensions of Au/TiO_2−M under irradiation of visible light.

CONCLUSIONS

By using traditional photodeposition of various metal cocatalysts (M) on nanocrystalline TiO_2 followed by colloid photodeposition of Au particles onto TiO_2−M, Au/TiO_2−M samples without alloying Au and M and nanoparticle coagulation were successfully prepared. The amounts of Au and M fixed onto TiO_2 can be changed independently, and various homemade and commercially available TiO_2 samples were used as supports for Au and M. The Au/TiO_2 and Au/TiO_2−Pt samples exhibited strong photoabsorption around 550 nm due to SPR of Au particles and yielded H_2 from 2-propanol in aqueous solutions under irradiation of visible light of a xenon lamp filtered with a Y-48 filter. Since bare TiO_2 and TiO_2−Pt

dx.doi.org/10.1021/cs3006499 | ACS Catal. 2013, 3, 79−85

yielded no H_2 under the same conditions, we concluded that SPR photoabsorption of supported Au particles contributed to the H_2 evolution under irradiation of visible light. The Au/TiO_2−Pt sample exhibited a rate of H_2 formation ∼7-times larger than that of the Pt-free Au/TiO_2 sample, indicating that Pt nanoparticles loaded onto TiO_2 acted effectively as reduction sites for H_2 evolution. The H_2 formation rates of the Au/TiO_2−M samples depended on the kind of M and decreased in the order of M: Pt > Pd > Ru > Rh > Au > Ag > Cu > Ir. An inverse correlation between the rates and the HOV values indicates that each M in the Au/TiO_2−M sample actually acted as a site for H^+ reduction (H_2 formation). The amount of Pt particles was one of the decisive factors determining the rate, and the maximum rate was obtained at 0.5 wt %. The amount of Au particles determined the intensity of SPR photoabsorption at 550 nm of Au/TiO_2−Pt samples, and a linear correlation was observed between the rate of H_2 formation and SPR photoabsorption (not the amount of Au particles). Introduction of Pt nanoparticles was effective for many kinds of Au/TiO_2 samples having various physical properties, and the H_2 formation rates were 5−9 times larger than that of the Pt-free Au/TiO_2 samples.

■ ASSOCIATED CONTENT

Supporting Information

TEM images of Au(1.0)/TiO_2−M(0.5) samples (M = Pd, Au, Ag, Rh, Ru). This material is available free of charge via the Internet at http://pubs.acs.org.

■ AUTHOR INFORMATION

Corresponding Author

*E-mail: hiro@apch.kindai.ac.jp.

Notes

The authors declare no competing financial interest.

■ ACKNOWLEDGMENTS

This work was supported in part by a Grant-in-Aid for Scientific Research (No. 23560935) from the Ministry of Education, Culture, Sports, Science, and Technology (MEXT) of Japan. The authors (H.K. and A.T.) are grateful for financial support from Iketani Science and Technology Foundation.

■ REFERENCES

(1) Kawai, T.; Sakata, T. *Nature* **1980**, *286*, 474−476.
(2) Fox, M. A.; Dulay, M. T. *Chem. Rev.* **1993**, *93*, 341−357.
(3) Hoffmann, M. R.; Martin, S. T.; Choi, W.; Bahnemann, D. W. *Chem. Rev.* **1995**, *95*, 69−96.
(4) Shimura, K.; Yoshida, H. *Energy Environ. Sci.* **2011**, *4*, 2467−2481.
(5) Kominami, H.; Nishimune, H.; Ohta, Y.; Arakawa, Y.; Inaba, T. *Appl. Catal., B* **2012**, *111−112*, 297−302.
(6) Yuzawa, H.; Mori, T.; Itoh, H.; Yoshida, H. *J. Phys. Chem. C* **2012**, *116*, 4126−4136.
(7) Fuku, K.; Kamegawa, T.; Mori, K.; Yamashita, H. *Chem.—Asian J.* **2012**, *7*, 1366−1371.
(8) Chen, X.; Shen, S.; Guo, L.; Mao, S. S. *Chem. Rev.* **2010**, *110*, 6503−6570.
(9) Navarro, R. M.; Sánchez-Sánchez, M. C.; Alvarez-Galvan, M. C.; del Valle, F.; Fierro, J. L. G. *Energy Environ. Sci.* **2009**, *2*, 35−54.
(10) Tian, Y.; Tatsuma, T. *J. Am. Chem. Soc.* **2005**, *127*, 7632−7637.
(11) Furube, A.; Du, L.; Hara, K.; Katoh, R.; Tachiya, M. *J. Am. Chem. Soc.* **2007**, *129*, 14852−14853.
(12) Naya, S.; Teranishi, M.; Isobe, T.; Tada, H. *Chem. Commun.* **2010**, *46*, 815−817.
(13) Kowalska, E.; Abe, R.; Ohtani, B. *Chem. Commun.* **2009**, 241−243.
(14) Kowalska, E.; Mahaney, O. O. P.; Abe, R.; Ohtani, B. *Phys. Chem. Chem. Phys.* **2010**, *12*, 2344−2355.
(15) Silva, C. G.; Juarez, R.; Marino, T.; Molinari, R.; Garcia, H. *J. Am. Chem. Soc.* **2011**, *133*, 595−602.
(16) Yuzawa, H.; Yoshida, T.; Yoshida, H. *Appl. Catal., B* **2012**, *115*, 294−302.
(17) Ke, X.; Sarina, S.; Zhao, J.; Zhang, X.; Chang, J.; Zhu, H. *Chem. Commun.* **2012**, *48*, 3509−3511.
(18) Linic, S.; Christopher, P.; Ingram, D. B. *Nat. Mater.* **2011**, *10*, 911−921.
(19) Warren, S. C.; Thinsen, E. *Energy Environ. Sci.* **2012**, *5*, 5133−5146.
(20) Zhou, X.; Liu, G.; Yu, J.; Fan, W. *J. Mater. Chem.* **2012**, *22*, 21337−21354.
(21) Kominami, H.; Tanaka, A.; Hashimoto, K. *Chem. Commun.* **2010**, *46*, 1287−1289.
(22) Kominami, H.; Tanaka, A.; Hashimoto, K. *Appl. Catal., A* **2011**, *397*, 121−126.
(23) Tanaka, A.; Hashimoto, K.; Kominami, H. *ChemCatChem* **2011**, *3*, 1619−1623.
(24) Tanaka, A.; Hashimoto, K.; Kominami, H. *Chem. Commun.* **2011**, *47*, 10446−10448.
(25) Tanaka, A.; Sakaguchi, S.; Hashimoto, K.; Kominami, H. *Catal. Sci. Technol.* **2012**, *2*, 907−909.
(26) Tanaka, A.; Hashimoto, K.; Kominami, H. *J. Am. Chem. Soc.* **2012**, *134*, 14526−14533.
(27) Tanaka, A.; Ogino, A.; Iwaki, M.; Hashimoto, K.; Ohnuma, A.; Amano, F.; Ohtani, B.; Kominami, H. *Langmuir* **2012**, *28*, 13105−13111.
(28) Kominami, H.; Kohno, M.; Takada, Y.; Inoue, M.; Inui, T.; Kera, Y. *Ind. Eng. Chem. Res.* **1999**, *38*, 3925−3931.
(29) Kominami, H.; Murakami, S.-y.; Kato, J.-i.; Kera, Y.; Ohtani, B. *J. Phys. Chem. B* **2002**, *106*, 10501−10507.
(30) Frens, G. *Nat. Phys. Sci.* **1973**, *241*, 20−22.
(31) Kominami, H.; Furusho, A.; Murakami, S.-Y.; Inoue, H.; Kera, Y.; Ohtani, B. *Catal. Lett.* **2001**, *76*, 31−34.
(32) Christopher, P.; Ingram, D. B.; Linic, S. *J. Phys. Chem.* **2010**, *114*, 9173−9177.